horticulturae

MDPI

Article

Genome-Wide Identification of Watermelon Trihelix Genes and Their Expression Patterns Under Biotic and Abiotic Stresses

Yunan Wang [1,2], Hui Cheng [1,2], Zhonghao Liang [1], Yuting Su [1], Lijing Shi [1] and Nannan Qin [1,3,*]

[1] College of Horticulture, Shanxi Agricultural University, Jinzhong 030801, China; wangyunan168@163.com (Y.W.); shl2004@126.com (H.C.); liangzhonghao2711@163.com (Z.L.); suyuting11111@163.com (Y.S.); shilijing20002@163.com (L.S.)
[2] Department of Scientific Research Management, Shanxi Agricultural University, Taiyuan 030031, China
[3] Department of Development Planning & Cooperation, Shanxi Agricultural University, Taiyuan 030031, China
* Correspondence: nnqnews@163.com

Abstract: Trihelix transcription factors (TFs) play crucial roles in plant growth, development, and environmental adaptation. However, there have been no systematic studies on the trihelix gene family in watermelon (*Citrullus lanatus*). A comprehensive study of trihelix genes in watermelon could provide new insights into its evolution and breeding potential. In this study, we identified 29 watermelon trihelix genes and analyzed their genome-wide information, molecular evolution, and expression patterns. The 29 watermelon trihelix genes were distributed across 12 chromosomes and grouped into five subfamilies. Evolutionary analysis revealed that four watermelon trihelix genes were collinear with six trihelix genes in *Arabidopsis thaliana*, and 20 watermelon trihelix genes were collinear with 20 trihelix genes in cucumber (*Cucumis sativus*). Gene duplication event analysis suggested that the expansion of the trihelix gene family mainly occurred through segmental duplications. Gene expression analysis showed distinct expression patterns of trihelix genes in watermelon, with evidence of tissue-specific expression. Furthermore, expression pattern analysis of watermelon trihelix genes in response to stress revealed that the *Cla97C10G2055470* gene was associated with the response to salt stress, while the *Cla97C06G127520* gene was associated with watermelon resistance to SqVYV disease. In conclusion, the phylogenetic, evolutionary, and expression analyses of the trihelix gene family in watermelon provide a solid foundation for future functional studies.

Keywords: trihelix gene family; *Citrullus lanatus*; evolutionary analysis; expression pattern analysis

check for updates

Academic Editor: Yuyang Zhang

Received: 16 December 2024
Revised: 25 February 2025
Accepted: 3 March 2025
Published: 4 March 2025

Citation: Wang, Y.; Cheng, H.; Liang, Z.; Su, Y.; Shi, L.; Qin, N. Genome-Wide Identification of Watermelon Trihelix Genes and Their Expression Patterns Under Biotic and Abiotic Stresses. *Horticulturae* **2025**, *11*, 275. https://doi.org/10.3390/horticulturae11030275

Copyright: © 2025 by the authors. Licensee MDPI, Basel, Switzerland. This article is an open access article distributed under the terms and conditions of the Creative Commons Attribution (CC BY) license (https://creativecommons.org/licenses/by/4.0/).

1. Introduction

Plant transcription factors (TFs) play a crucial role in regulating gene expression, determining how cells utilize their genetic information. By binding to specific DNA sequences, typically located in gene promoters or enhancers, they control the level of gene transcription, ultimately influencing protein production. Currently, more than 60 TF families have been identified in plants, and the functions of a substantial number of these TFs have either been fully defined or are gradually being clarified [1]. As one of the TF families discovered in plants, the trihelix TF family has been increasingly studied in recent years.

Members of the trihelix TF family possess a classic trihelix (helix–loop–helix–loop–helix) domain, which specifically binds to the GT elements of the DNA sequence involved in the light response, earning them the classification as GT factors [2,3]. The first identified

trihelix gene, *GT-1*, was found in pea (*Pisum sativum*) [4], and its homologous genes were subsequently cloned in tobacco and *Arabidopsis* [5,6]. Trihelix genes have since been detected in several major plants, including rice (*Oryza sativa*) [7], soybean (*Glycine max*) [8], tomato (*Solanum lycopersicum*) [9], and chrysanthemum (*Chrysanthemum morifolium*) [10]. Based on the structure of the trihelix domain, trihelix TFs are categorized into five clades: GT-1, GT-2, SH4, GTγ, and SIP1 [11].

In recent years, an increasing number of trihelix genes have been cloned and characterized. Previous studies have found that trihelix TFs are indeed involved in plant responses to both biotic and abiotic stresses. Maréchal et al. [12] found that the induction of the *GT-1* gene by light may depend on its phosphorylation, as the phosphorylation of a threonine in the trihelix domain increased the binding strength of GT-1 to its target by 10 to 20 times. The *Arabidopsis GT-2 LIKE 1* (*GTL1*) TF negatively regulates water use efficiency (WUE) by transrepressing *SDD1*, thereby increasing stomatal conductance. When GTL1 function was lost, stomatal density was decreased, and WUE was increased, without altering CO_2 assimilation, thereby enhancing tolerance to water deficit stress [13]. In addition, Shibata et al. [14] combined transcriptomic data with whole-genome chromatin binding data to demonstrate that GTL1 and DF1 directly bind to the *ROOT HAIR DEFECTIVE SIX-LIKE4* (*RSL4*) activator and regulate its expression to inhibit root hair growth. AtGT2L is a Ca^{2+}/CaM-binding nuclear TF involved in plant responses to cold and salt stresses. Under chilling/NaCl stress, the cold- and salt-induced marker genes *RD29A* and *ERD10* exhibited significantly higher expression levels in *Arabidopsis* plants overexpressing *AtGT2L* [15]. Overexpression of *BnSIP1-1*, which belongs to the *SIP1* (*6b INTERACTING PROTEIN1*) trihelix clade, significantly enhanced seed germination under osmotic pressure, salt, and abscisic acid treatments [16]. Fu et al. [17] found that SlGT31 can bind to the promoters of two key ethylene biosynthesis genes, *ACO1* and *ACS4*, and overexpression of the *SlGT31* gene can significantly accelerate tomato fruit ripening. Additionally, MdSIP1-2 can directly bind to the GT1 motif of the *MdNIR1* promoter, inhibiting its transcription, which leads to a reduced rate of nitrate utilization in apple (*Malus domestica*) [18]. All these results indicate that different trihelix TFs exhibit specific functions in different crops. With the advancement of science and technology, an increasing number of plant trihelix genes have been studied, including those in *Populus trichocarpa* [19], *Gossypium arboretum* [20], wheat (*Triticum aestivum*) [21], and rice [22]. However, there has not yet been a systematic study of trihelix genes in watermelon (*Citrullus lanatus*).

Watermelon is a globally significant crop due to its high nutritional value and economic importance, particularly in regions with warm climates, including China, which is one of the largest producers. Watermelon faces various challenges during production, including climate change, pests and diseases, soil salinization, and water resource shortages, all of which severely impact its growth and yield. Additionally, watermelon has relatively weak resistance to certain pests and diseases, making it susceptible to attacks from diseases such as powdery mildew and downy mildew. Transcription factors (TFs) play crucial roles in watermelon's response to both biotic and abiotic stresses by regulating gene expression involved in stress tolerance mechanisms [23,24]. In this context, the importance of studying stress resistance genes has become increasingly prominent. Therefore, this study systematically and comprehensively identified the trihelix genes in watermelon on a genome-wide scale and analyzed their physicochemical properties, chromosomal localization, gene structure, and phylogeny. Based on transcriptome sequencing data, we performed tissue-specific expression analysis of all trihelix genes in watermelon. In addition, we investigated the expression patterns of trihelix genes in response to biotic and abiotic stress. These results lay an important foundation for further research on the

functions of trihelix TFs in watermelon and provide a theoretical reference for the molecular breeding of watermelon.

2. Materials and Methods

2.1. Identification and Physicochemical Property Analysis of Watermelon Trihelix Genes

The hidden Markov model (HMM) file (PF02704) of the trihelix gene family was downloaded from the Pfam database (https://www.ebi.ac.uk/interpro/, accessed on 16 July 2024), and potential trihelix genes were scanned using HMMER 3.0 (E-value < 1×10^{-5}). Pfam and SMART (https://smart.embl.de/smart/batch.pl, accessed on 15 July 2024) were used to identify trihelix genes, with genes containing trihelix domains recognized as trihelix genes [25]. The physicochemical characteristics of all watermelon trihelix proteins—including the number of amino acids, molecular weight, isoelectric point, instability index, aliphatic index, and grand average of hydropathicity—were explored using the online tool ExPASy (https://web.expasy.org/protparam/, accessed on 16 July 2024). The subcellular localization of all trihelix genes was predicted through the online website CELLO (http://cello.life.nctu.edu.tw/, accessed on 16 July 2024) [26] and visualized using TBtools v2.056 software [27].

2.2. Structural Analysis and Phylogenetic Tree Construction of Watermelon Trihelix Genes

The structure of watermelon trihelix genes was analyzed using the online tool GSDS 2.0 (https://gsds.gao-lab.org/, accessed on 16 July 2024) based on the GFF3 (general feature format 3) file. The conserved motif of trihelix proteins was analyzed using the online software MEME (http://meme-suite.org/, accessed on 16 July 2024) [28], with the number of conserved motifs set as 10 and the optimal match length set as 6–200 amino acid residues. Multiple sequence alignment was performed using ClustalX 2.0 and visualized using Jalview Version 2 [29]. A phylogenetic tree was constructed using MEGA7 [30] with the neighbor-joining method using the Poisson model, pairwise deletion, and 1000 bootstrap replications [31].

2.3. Synteny Analyses of Trihelix Genes

The intraspecific and interspecific gene duplication events of the watermelon trihelix gene family were analyzed using the Multiple Collinearity Scan toolkit (MCScanX 1.0.0) with the default parameters [32]. Syntenic analysis maps were constructed using Dual Systeny Plotter (https://github.com/CJ-Chen/TBtools-II, accessed on 18 July 2024). Furthermore, candidate homologous gene pairs identified from the same synteny block were used as the input for the software KaKs_Calculator 2.0 to calculate the Ka and Ks values [33].

2.4. RNA-Seq Re-Analysis of Transcriptome Sequencing Data

The transcriptome sequencing data were downloaded from the NCBI database (https://www.ncbi.nlm.nih.gov/, accessed on 22 July 2024), and then the SRA data were converted to fastq data using fasterq-dump.2.11.0 (https://github.com/ncbi/sra-tools/wiki/HowTo:-fasterq-dump, accessed on 23 July 2024). The quality of data was checked using FastQC v0.11.9 [34], and the Trimmomatics plugin was used to remove adapters and low-quality sequences [35] to obtain filtered clean data. The filtered transcriptome data were compared to the watermelon genome using STAR. BAM files were generated [36], and gene expression was analyzed, using the StringTie 2.2.1 software [37]. Then, differentially expressed genes (DEGs) were determined using the DESeq2 1.0.3 software [38].

2.5. Tissue-Specific Expression Analysis of Watermelon Trihelix Genes

The transcriptome sequencing project PRJNA1031825 [39] was downloaded from the SRA database to screen the expression pattern of trihelix genes in different tissues, including the root of one-true-leaf stage, stem, stem of the one-true-leaf stage, male flower, female flower, fruit, leaf, and tendril. TBtools was used to draw a heatmap of the expression patterns of trihelix genes in different watermelon tissues.

2.6. Analysis of Expression Patterns Under Abiotic and Biotic Stresses

The transcriptome sequencing projects performed under high temperature (PRJNA1031825), low temperature (PRJNA328189) [40], salt (PRJNA609260) [41], drought (PRJNA326331) [42], *Fusarium* wilt (PRJNA973274), powdery mildew (PRJNA881394) [43], *Cucumber Green Mottle Mosaic Virus* (CGMMV; PRJNA534308) and *Squash Vein Yellowing Virus* (SqVYV; PRJNA086032) stresses were downloaded from the SRA database, and the expression pattern of watermelon trihelix genes was analyzed. Similar to above, the heatmaps were drawn using TBtools.

2.7. RNA Extraction and Gene Expression Analysis

The cultivar 8424 (*Citrullus lanatus*) were used to explore gene expression under high temperature and salt stress. Watermelon seedlings (two-leaf and one-heart stage) were exposed to short-term salt stress (300 mM NaCl), with distilled water as the control. After 7 h of exposure to salt stress, leaf samples were collected stored at −80 °C. At the same time, the watermelon seedlings were treated with 45 °C high temperature, and the leaves of the seedlings were collected at 0, 4, 8, 12, and 24 h after treatment for RT-qPCR. All treatments were carried out in a controlled climate chamber as used in previous transcriptomic studies. Total RNA was isolated using the RNAprep Pure Plant Kit (DP432; Tiangen Biotech, Beijing, China) following the manufacturer's protocol. Total of 1 μg RNA was reverse transcribed into cDNA using the PrimeScript RT Kit (Takara, Kyoto, Japan). Specific primers for each gene were designed using Primer 6 (Table 1). The resulting cDNA was then analyzed via RT-qPCR using SYBR Green PCR Master Mix (Vazyme, Nanjing, China) on an Opticon thermocycler (CFX96 Connect Real-Time PCR System; Bio-Rad, Hercules, CA, USA) according to the manufacturer's guidelines. Relative expression levels were determined using the $2^{-\Delta\Delta CT}$ method and presented as $\log_2$ fold change (FC) compared to the control. Data analysis was carried out using Excel 2024.

Table 1. The primers of 8 selected watermelon trihelix genes used for the real time quantitative PCR analysis.

Gene Name	Forward Primer (5′-3′)	Reverse Prime (5′-3′)	Size (bp)
Actin	CCATGTATGTTGCCATCCAG	GGATAGCATGGGGTAGAGCA	135
Cla97C05G083690	GAATCTCAAGGCTACTCACT	CTCCATCTTATGACGACACT	106
Cla97C05G109140	CCGCCATGTCTCTTCAAG	CGGAGGCAGATTCAGAAC	110
Cla97C08G147040	CTCCACTACTTCCGTCTTG	TCATCCTCACCAGAATTGTT	126
Cla97C08G147050	AGTGGGAAATCCGATAACAG	GGTGGTGGTGAGATTGGA	115
Cla97C09G164310	AGACAACAAGCAGAACAGT	GCATACGAGGAGCAAGTT	113
Cla97C09G171740	AGCATCAGCAACATACTCC	CCTCTTCTTCTTCTTCCTCTT	103
Cla97C10G197980	GTTGGGACCCTGTATTGG	TCTCGTAATGTGGACATCC	114
Cla97C10G205470	CCATTCTACACAGAGTTACAAG	TTCTTCGTCATCGTCAGAC	129

3. Results

3.1. Identification and Physicochemical Characteristics of Watermelon Trihelix Genes

A total of 29 trihelix gene family members were identified in the watermelon genome, distributed across 11 chromosomes. As Figure S1 shows, all the 29 trihelix genes have evolved conserved structural domains, once again proving the accuracy of the identification. The trihelix genes were unevenly distributed across the chromosomes; for example, there were five genes on chromosome 10, while chromosomes 3, 4, and 11 each had only one gene (Figure 1).

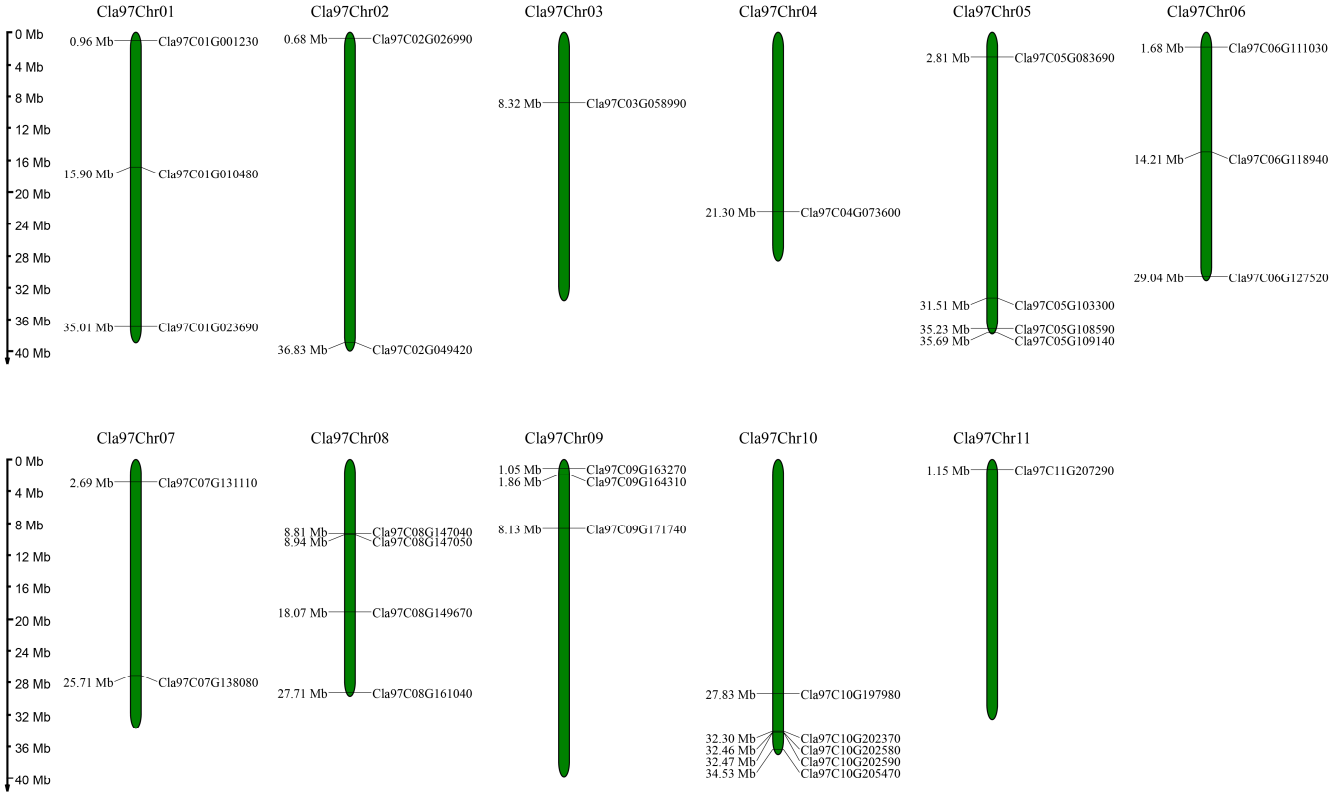

Figure 1. Distribution of trihelix family genes in the watermelon genome.

The coding sequence (CDS) length of the 29 trihelix genes ranged from 300 to 2712 bp, encoding proteins with lengths from 99 to 903 amino acids (aa). Their molecular weight ranged from 11.73 to 101.54 kD, with isoelectric points between 4.81 and 9.67. Among them, eight watermelon trihelix proteins were basic proteins, while the remaining 21 trihelix proteins were acidic proteins. The aliphatic index ranged from 50.03 to 86.78, and the instability index ranged from 42.29 to 74.28. All of the trihelix proteins were unstable (instability index greater than 40). The grand average of hydropathy (GRAVY) values ranged from −1.26 to −0.381, with all proteins being hydrophobic (GRAVY < 0). Subcellular localization predictions showed that 28 trihelix proteins were located in the nucleus, while one (*Cla97C10G202580*) was located in plasma membrane (Table 2). Subsequently, 29 trihelix genes were named *ClGT1* to *ClGT29* according to their order on the chromosomes.

Table 2. The physicochemical characteristics of the 29 watermelon trihelix genes.

Gene ID	Name	CDS Size (bp)	Number of Amino Acids (aa)	Molecular Weight (kD)	pI	Instability Index	Aliphatic Index	Grand Average of Hydro-pathic-ity	Prediction of Subcellular Location
Cla97C01G001230	*ClGT1*	2091	696	77.00	5.05	69.59	57.44	−0.827	Nuclear
Cla97C01G010480	*ClGT2*	1473	490	55.20	5.86	60.44	68.88	−0.701	Nuclear
Cla97C01G023690	*ClGT3*	1386	461	51.39	8.94	54.43	73.38	−0.633	Nuclear
Cla97C02G026990	*ClGT4*	1473	490	56.13	5.55	51.33	62.76	−1.025	Nuclear
Cla97C02G049420	*ClGT5*	1275	424	48.04	6.74	50.98	66.65	−0.826	Nuclear
Cla97C03G058990	*ClGT6*	936	311	34.96	5.74	47.88	66.24	−0.629	Nuclear
Cla97C04G073600	*ClGT7*	300	99	11.73	9.51	48.06	70	−0.705	Nuclear
Cla97C05G083690	*ClGT8*	1083	360	39.75	9.33	66.93	52.36	−0.919	Nuclear
Cla97C05G103300	*ClGT9*	1233	410	46.50	6.38	47.81	54.73	−0.874	Nuclear
Cla97C05G108590	*ClGT10*	2712	903	101.54	5.79	42.65	83.93	−0.521	Nuclear
Cla97C05G109140	*ClGT11*	1053	350	38.86	9.59	63.59	61.63	−0.962	Nuclear
Cla97C06G111030	*ClGT12*	1068	355	38.67	5.4	50.41	75.61	−0.642	Nuclear
Cla97C06G118940	*ClGT13*	1872	623	72.13	5.99	62.88	61.36	−1.159	Nuclear
Cla97C06G127520	*ClGT14*	2709	902	99.89	8.71	46.03	86.78	−0.381	Nuclear
Cla97C07G131110	*ClGT15*	858	285	32.33	9.56	48.74	75.61	−0.615	Nuclear
Cla97C07G138080	*ClGT16*	978	325	38.06	8.67	57.83	61.05	−1.003	Nuclear
Cla97C08G147040	*ClGT17*	1920	639	71.53	6.06	69.98	55.27	−1.052	Nuclear
Cla97C08G147050	*ClGT18*	1638	545	61.81	5.66	64.55	51.89	−1.096	Nuclear
Cla97C08G149670	*ClGT19*	1401	466	52.78	6.36	42.29	67.58	−0.893	Nuclear
Cla97C08G161040	*ClGT20*	1224	407	46.61	5.83	53.11	61.84	−0.826	Nuclear
Cla97C09G163270	*ClGT21*	1128	375	41.20	9.67	46.21	59.04	−0.97	Nuclear
Cla97C09G164310	*ClGT22*	1161	386	44.45	4.81	50.15	50.03	−1.26	Nuclear
Cla97C09G171740	*ClGT23*	921	306	35.41	5.38	74.28	64.12	−0.925	Nuclear
Cla97C10G197980	*ClGT24*	981	326	37.76	6.97	46.64	66.44	−0.839	Nuclear
Cla97C10G202370	*ClGT25*	1575	524	59.43	6.53	49.59	52.6	−1.087	Nuclear
Cla97C10G202580	*ClGT26*	1815	604	66.90	6.43	44.84	73.44	−0.408	PlasmaMembrane
Cla97C10G202590	*ClGT27*	1554	517	58.09	5.8	62.93	57.16	−0.969	Nuclear
Cla97C10G205470	*ClGT28*	915	304	35.54	6.82	52.11	55.59	−1.128	Nuclear
Cla97C11G207290	*ClGT29*	1197	398	44.88	9.02	71.04	61.31	−0.951	Nuclear

3.2. Evolutionary Analysis of Trihelix Genes Among Different Species

To clarify the phylogenetic relationships of the trihelix genes among watermelon and other crops, a phylogenetic tree was constructed including *Arabidopsis* [44] and cucumber (*Cucumis sativus*) [45]. The trihelix proteins of the three plants were divided into five subfamilies (Figure 2). Subfamily SIP1 was the largest, containing 12 trihelix proteins from *Arabidopsis*, 10 from cucumber, and 11 from watermelon. Subfamily GT2 was next, with seven from *Arabidopsis*, seven from cucumber, and eight from watermelon. Subfamily GTγ had the fewest trihelix proteins, including those from cucumber, *Arabidopsis*, and watermelon. The distribution of these genes could indicate their paralogous or orthologous relationships among the three plants. The clustering of orthologous genes suggests that these genes may be functionally conserved; for example, the orthologous relationships between genes in Cucurbitaceae crops are relatively close. Conversely, the genetic divergence between species indicates functional diversification of trihelix proteins throughout the evolutionary process in different species.

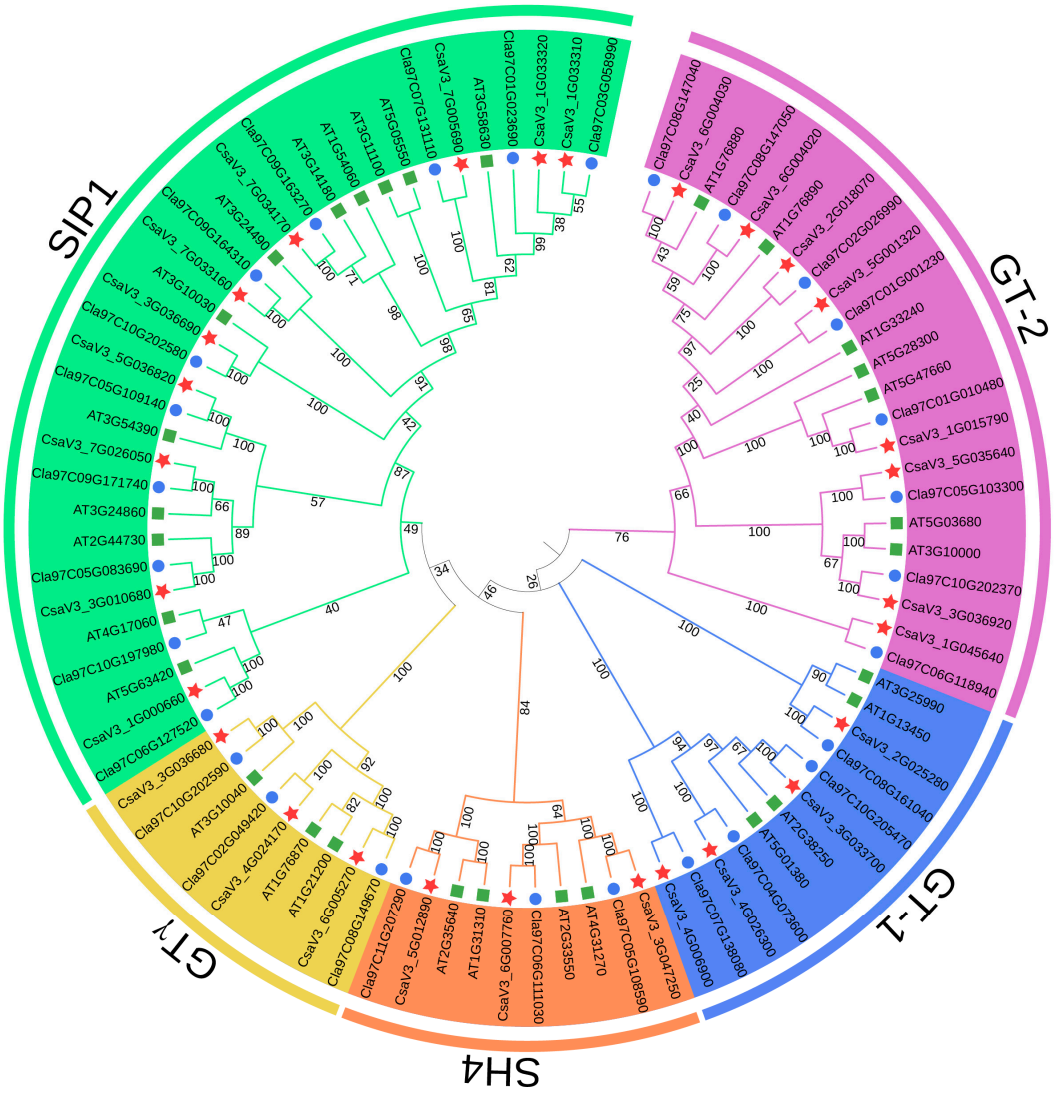

Figure 2. Phylogenetic analysis of trihelix proteins from *C. sativus* and *Arabidopsis*.

3.3. Structure and Conserved Sequence Analysis of Trihelix Genes

A phylogenetic tree was constructed for the watermelon trihelix gene family, and the 29 trihelix family members were divided into five branches: *GT-1*, *GT-2*, *SH4*, *GTγ*, and *SIP1* (Figure 3). The results of the motif prediction analysis indicated that with a limit of 10 motifs, none of the trihelix genes contained all motifs. Motif 1 was the most conserved and appeared in all trihelix genes. The conserved motifs were unevenly distributed among the various trihelix genes. For example, there were seven conserved motifs in *Cla97C08G147040* but only two in *Cla97C10G197980*. Most genes within the same evolutionary branch exhibited the same conserved motifs. Gene structure analysis revealed that the number of exons in trihelix genes varied considerably, ranging from 1 to 17, indicating that the trihelix TFs have taken on different biological functions during the evolutionary process. Trihelix genes within the same lineage generally had similar structures, indicating a certain degree of conservation in motifs and structure within the same evolutionary branch.

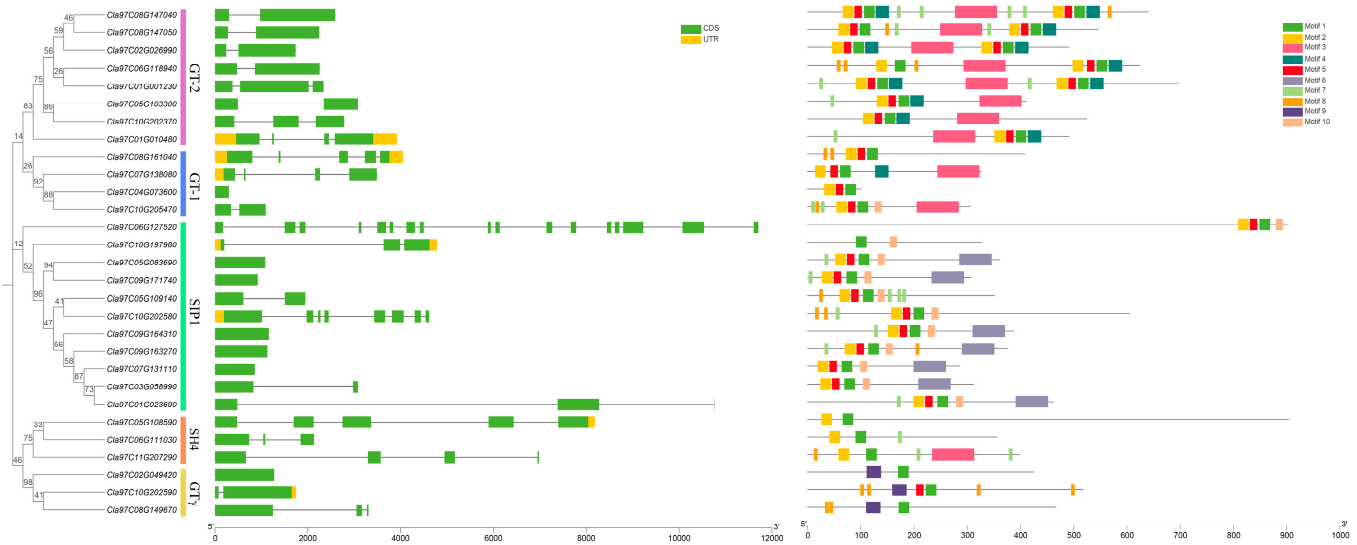

Figure 3. Exon–intron structures of trihelix genes and a schematic plot of the amino acid motifs of trihelix proteins in watermelon.

3.4. Intraspecies and Interspecies Synteny Analysis of Trihelix Genes

To investigate the evolution of the trihelix gene family, an intraspecies and interspecies synteny analysis was conducted. The results showed that three fragment duplication events (*Cla97C01G023690*:*Cla97C07G131110*, *Cla97C03G058990*:*Cla97C07G131110*, *Cla97C04G073600*:*Cla97C10G205470*) occurred in the trihelix gene family of watermelon (Figure 4). These results suggest that segmental duplication contributed to the expansion of the trihelix gene family. To further determine whether positive selection or purifying selection processes have driven the evolution of the trihelix gene family in watermelon, the Ka/Ks ratio of homologs was calculated using the CDS of trihelix genes. Each segmental duplication gene pair had a Ka/Ks ratio less than one (Table 3), indicating that purifying selection was the primary driver of trihelix gene evolution in watermelon.

Table 3. Ka/Ks ratio of watermelon trihelix gene homologs.

Homologs Genes	Ka	Ks	Ka/Ks	*p*-Value
Cla97C01G023690-Cla97C07G131110	0.452	3.845	0.118	2.912×10^{-25}
Cla97C03G058990-Cla97C07G131110	0.470	3.849	0.122	2.355×10^{-36}
Cla97C04G073600-Cla97C10G205470	0.392	3.084	0.127	1.776×10^{-15}

To further infer the phylogenetic mechanisms of the watermelon trihelix family, a collinearity map was constructed in relation to *Arabidopsis* and cucumber. Four watermelon trihelix genes exhibited six kinds of collinear relationships with six trihelix genes in *Arabidopsis*, while 22 watermelon trihelix genes showed 22 kinds of collinear relationships with 22 trihelix genes in cucumber (Figure 5). This indicates that these orthologous gene pairs may have existed before the ancestral divergence.

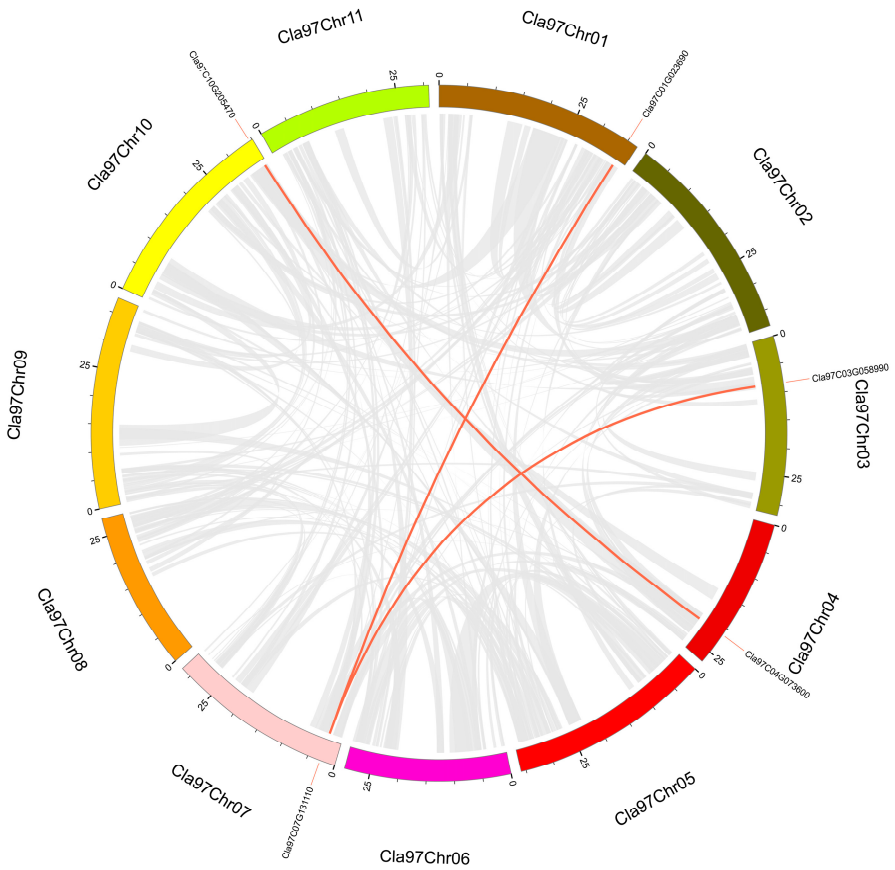

Figure 4. Collinear relationships among watermelon trihelix genes.

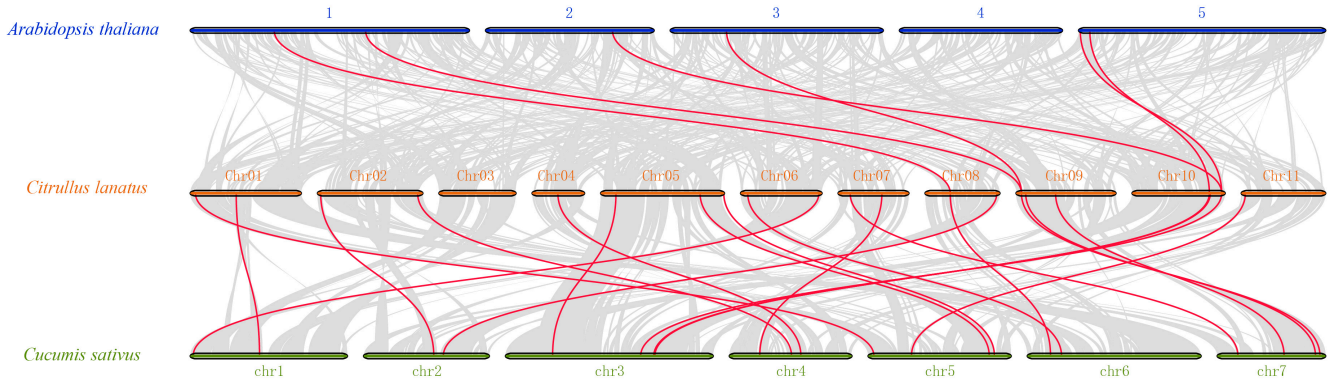

Figure 5. Syntenic analysis of the trihelix genes among watermelon, cucumber, and *Arabidopsis*. The gray lines in the background indicated the collinear blocks within the watermelon, cucumber, and *Arabidopsis* genomes, the red lines indicated the homologous gene pairs of trihelix family genes.

3.5. Tissue-Specific Expression Patterns of Watermelon Trihelix Genes

Based on the RNA-Seq results, the expression levels of watermelon trihelix genes were studied in eight different tissues or organs: root of the one-true-leaf stage, stem, stem of the one-true-leaf stage, male flower, female flower, fruit, leaf, and tendril (Figure 6). Six trihelix genes exhibited high expression levels in all tissues, such as *Cla97C02G026990* and *Cla97C09G163270* genes. Four genes displayed low expression levels across all tissues, such as *Cla97C01G010480* and *Cla97C05G108590* genes. However, some genes showed significant differences in expression among different tissues. For example, the *Cla97C08G147050* gene had high expression levels in tendrils but lower expression levels in leaves and male flowers. *Cla97C10G205470* gene exhibited high expression levels only in the root of the one-true-leaf stage, with low expression levels in other tissues. In summary, the results indicated that

watermelon trihelix genes play different roles during the development of different tissues or organs and fulfill multiple functions in plant growth and development.

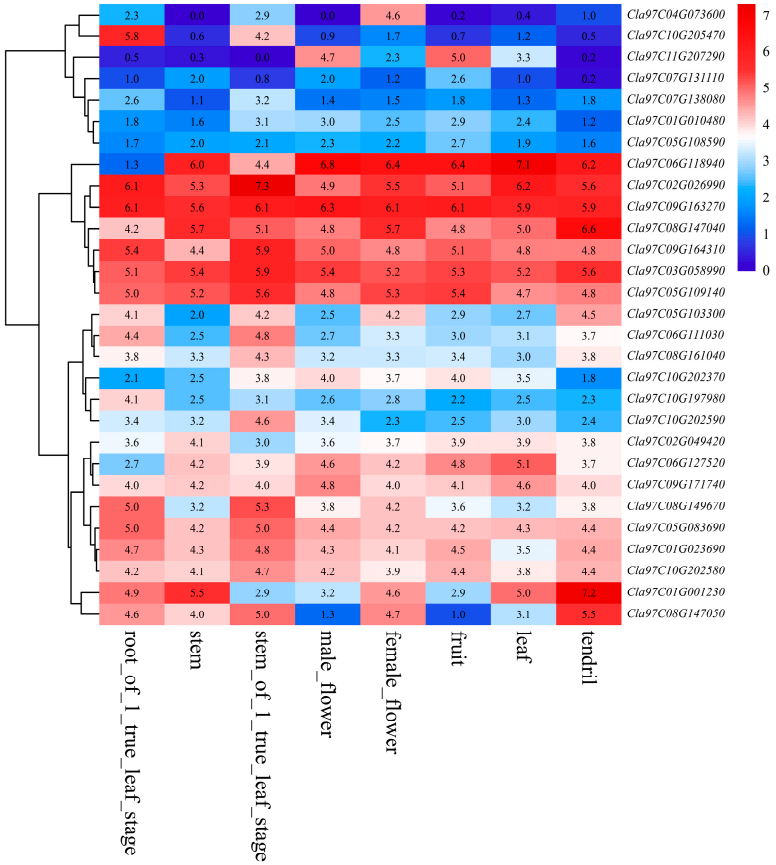

Figure 6. Heatmap of the expression patterns of watermelon trihelix gene family in different tissues and organs. In each figure, the color scale represents the level of expression, with red indicating high expression, and the deeper the color, the higher the expression. Blue represents low expression, and the deeper the color, the lower the expression. The numbers in the table represent the $\log_2$(FPKM + 1) values.

3.6. Expression Patterns of Watermelon Trihelix Genes Under Different Abiotic Stresses

Based on the public transcriptome data from the NCBI SRA database, the expression levels of watermelon trihelix genes under abiotic stress conditions (high temperature, low temperature, salt, and drought) were analyzed. Under high-temperature stress, most genes did not show significant differential expression after high-temperature treatment compared to the control. However, two genes exhibited differential expression patterns. *Cla97C08G19147040* gene exhibited gradually increasing expression levels with longer high-temperature treatment times. In contrast, the *Cla97C10G197980* gene showed a continuous decline in expression as the duration of high-temperature treatment increased. These results indicated that the *Cla97C08G19147040* and *Cla97C10G197980* genes were involved in the response to high-temperature stress, with *Cla97C08G19147040* having a positive response and *Cla97C10G197980* a negative response (Figure 7A). Under low-temperature stress, the expression levels of *Cla97C05G109140* and *Cla97C10G202580* genes were suppressed, while the remaining trihelix genes did not show significant differential expression. The results indicate that most trihelix TFs were not involved in the response to low-temperature stress (Figure 7B). Under salt stress, most trihelix genes did not show significant differential expression. However, the *Cla97C10G2055470* gene exhibited a significant increase in expression after salt treatment (Figure 7C). This result indicated that the *Cla97C10G2055470* gene actively responds to the high-salinity environment in watermelon. Under drought

stress, the expression level of the *Cla97C02G026990* gene increased after drought treatment, while the *Cla97C06G127520* gene showed suppressed expression after drought treatment (Figure 7D).

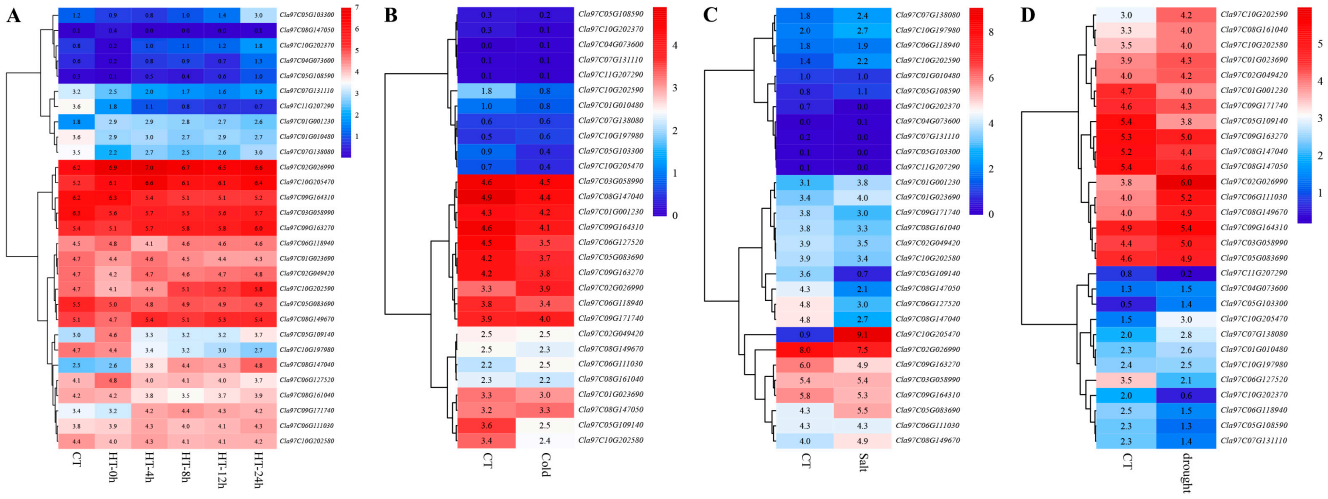

Figure 7. The expression heatmaps of watermelon trihelix gene family under abiotic stresses. (**A**) Expression heatmap of watermelon trihelix family genes under high-temperature stress. (**B**) Expression heatmap of watermelon trihelix family genes under low-temperature stress. (**C**) Expression heatmap of watermelon trihelix family genes under salt stress. (**D**) Expression heatmap of watermelon trihelix family genes under drought stress. In each figure, the color scale represents the level of expression, with red indicating high expression, and the deeper the color, the higher the expression. Blue represents low expression, and the deeper the color, the lower the expression. The numbers in the table represent the $\log_2$(FPKM + 1) values.

3.7. Expression Patterns of Watermelon Trihelix Genes Under Different Biotic Stresses

Under *Fusarium* wilt disease stress, most genes did not show differential expression between resistant and susceptible materials. After inoculation with *Fusarium* wilt pathogens, expression of the *Cla97C06G111030* gene was induced to high levels in susceptible materials, while no differential expression was found in resistant materials (Figure 8A). This result indicated that the trihelix gene family was not involved in the response of watermelon against *Fusarium* wilt disease. Under powdery mildew disease stress, most genes did not show differential expression between resistant and susceptible materials. After inoculation with powdery mildew, the *Cla97C06G118940* gene was suppressed in both resistant and susceptible materials. The *Cla97C08G161040* gene was induced to high levels, but the difference was not significant (Figure 8B). These results indicated that the trihelix gene family was not involved in the response to powdery mildew disease of watermelon. After infection by *Cucumber Green Mottle Mosaic Virus* (CGMMV), the expression levels of three genes (*Cla97C08G161040*, *Cla97C10G202580*, *Cla97C06G111030*) increased over time. At 25 d post-inoculation, their expression levels of these three trihelix genes were significantly upregulated. Compared to the control, the expression of the *Cla97C06G127520* gene showed no significant change at 48 h post-inoculation but was significantly downregulated at 25 d post-inoculation (Figure 8C). These results suggested that these four genes are involved in the response of cucumber to CGMMV infection. Under *Squash Vein Yellowing Virus* (SqVYV) stress, compared to the control, the expression of the *Cla97C10G205470* gene in susceptible plants gradually increased with inoculation time, reaching its peak at 15 dpi. However, in resistant plants, its expression did not significantly change within 10 dpi, only showing upregulation at 15 dpi. Additionally, the expression levels of the *Cla97C06G111030* and *Cla97C08G149670* genes gradually increased with time in both susceptible and resistant plants. *Cla97C06G127520* showed upregulation at 5 dpi in susceptible plants, but its

expression gradually decreased afterward. In resistant plants, the *Cla97C06G127520* gene was also upregulated at 5 dpi; however, unlike in susceptible plants, its expression remained significantly upregulated even at 10 dpi compared to the control (Figure 8D). These results suggested that the *Cla97C06G127520* gene may be involved in the molecular response to SqVYV of watermelon.

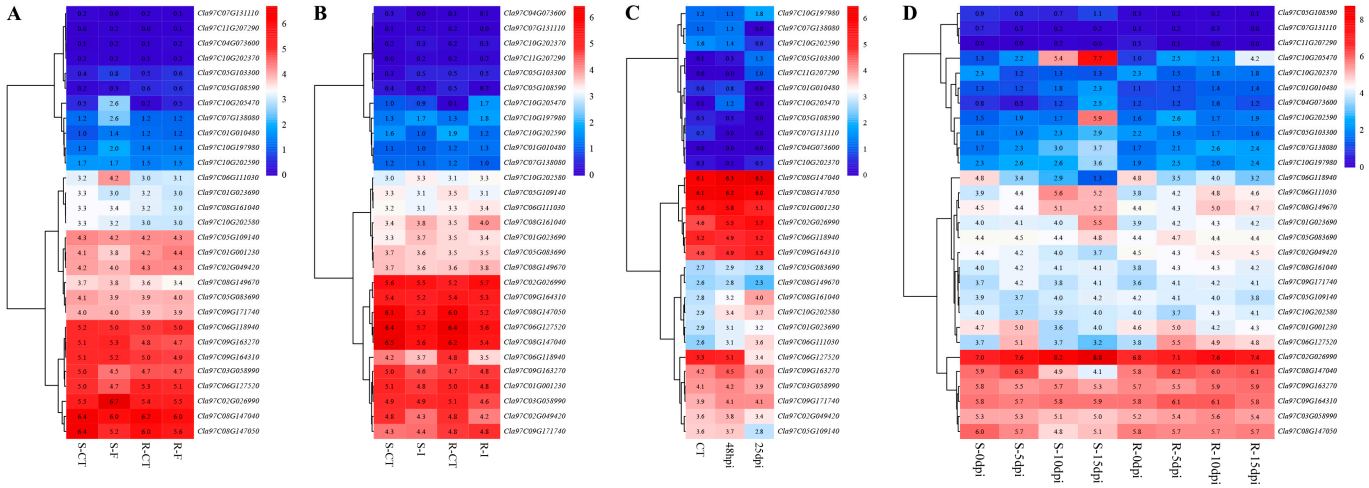

Figure 8. The expression heatmaps of watermelon trihelix gene family under biotic stresses. (**A**) Expression patterns of watermelon trihelix genes under *Fusarium* wilt stress. S-CT: the control of susceptible material; S-F: the susceptible material inoculated with *Fusarium* wilt disease; R-CT: the control of resistant material; R-F: the resistant material inoculated with *Fusarium* wilt disease. (**B**) Expression patterns of watermelon trihelix genes under powdery mildew stress. S-CT: the control of susceptible material; S-I: the susceptible material inoculated with powdery mildew disease; R-CT: the control of resistant material; R-I: the resistant material inoculated with powdery mildew disease. (**C**) Expression patterns of watermelon trihelix genes under CGMMV stress; CT: control; 48 hpi and 25 dpi were 48 h and 3 days post-inoculation, respectively. (**D**) Expression patterns of watermelon trihelix genes under SqVYV stress; S: susceptible plants; R: resistant plants; 0 dpi, 5 dpi, 10 dpi, and 15 dpi were 0, 5, 10, and 15 days post-inoculation, respectively. In each figure, the color scale represents the level of expression, with red indicating high expression, and the deeper the color, the higher the expression. Blue represents low expression, and the deeper the color, the lower the expression. The numbers in the table represent the $\log_2$(FPKM + 1) values.

3.8. Validation of Gene Transcription Expression

To further validate the RNA-Seq expression profile data, five watermelon trihelix genes (*Cla97C05G083690*, *Cla97C05G109140*, *Cla97C08G147040*, *Cla97C08G147050*, and *Cla97C10G205470*), which exhibited differential expression under salt stress, were selected for the RT-qPCR assays. The results showed that all five genes were consistent with respect to the expression profiles between the RT-qPCR analysis and the RNA-Seq data (Figure 9A,B). Similarly, we selected five differentially expressed watermelon trihelix genes (*Cla97C05G109140*, *Cla97C08G147040*, *Cla97C09G164310*, *Cla97C09G171740*, and *Cla97C10G197980*) under high-temperature stress for RT-qPCR validation. The results confirmed a high consistency with the RNA-Seq data (Figure 9C,D).

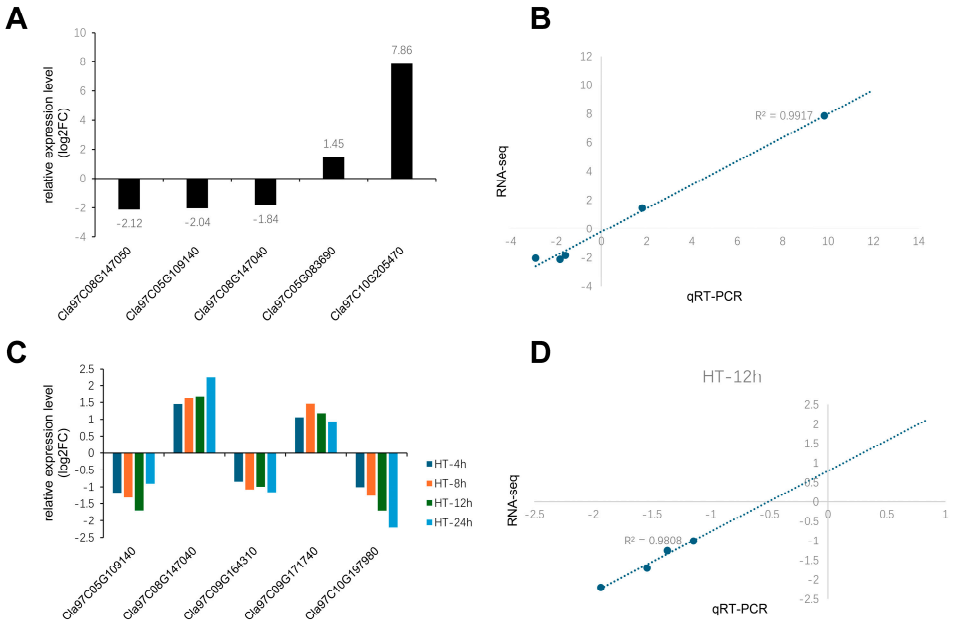

Figure 9. The gene expression and correlation analysis between RT-qPCR and RNA-Seq. (**A**) RT-qPCR analysis of 5 selected candidate genes under salt stress. (**B**) Correlation analysis of gene expression under salt stress between RNA-Seq and RT-qPCR. (**C**) RT-qPCR analysis of 5 selected candidate genes under high-temperature stress. (**D**) Correlation analysis of gene expression under high-temperature stress between RNA-Seq and RT-qPCR.

4. Discussion

In this study, 29 trihelix genes were identified in watermelon, which is similar to the number of trihelix genes in Arabidopsis (30) [44], but fewer than in rice (41) [22], soybean (63) [8], and tomato (36) [9]. This variation can likely be attributed to whole-genome duplication events that occurred after the divergence of these species from the earliest land plants. Such events introduced substantial genetic variation and enriched the genetic material, contributing to the plants' enhanced ability to adapt to diverse environments. Trihelix family proteins, as transcription factors (TFs), have been implicated in plant growth, development, and stress responses [15,46,47]. Early studies suggested that trihelix family genes could be classified into three main subfamilies: GTα, GTβ, and GTγ [48]. Building on this, Kaplan et al. classified trihelix genes into five clades based on their analysis of rice and Arabidopsis trihelix genes: GT-1, GT-2, SH4, GTγ, and SIP1 (Figure 3) [11]. In the present study, phylogenetic analysis revealed that watermelon trihelix genes can be grouped into five subfamilies, which is consistent with previous findings. Genes within the same subfamily share similar gene structures and motif compositions, suggesting a close evolutionary relationship. The analysis of gene duplication events identified three pairs of genes resulting from segmental duplications, supporting the idea that the expansion of trihelix genes mainly occurred through segmental duplications, as reported previously [49]. All Ka/Ks ratios for these gene pairs were less than 1 (Table 3), indicating that these duplicated genes have undergone strong purifying selection and likely subfunctionalization during evolution. This is consistent with findings that most duplicated genes in soybean have also been subfunctionalized [50]. Comparative analysis of trihelix genes among watermelon, cucumber, and Arabidopsis revealed that all homologous genes with a collinear relationship to Arabidopsis genes also exhibit collinearity with cucumber genes. However, in watermelon and cucumber, many homologous gene pairs did not share homology with Arabidopsis (Figure 5), suggesting that gene expansion occurred in a species-specific manner. This phenomenon has also been observed in other plant gene families [51,52].

The tissues in which genes are expressed typically reflect the functions of their corresponding proteins. *AT5G03680*, known as *Petal Loss* (*PTL*) in *Arabidopsis*, can inhibit the growth of sepal size, and the loss of the *PTL* gene can lead to a reduction in petal number [53]. In tomatoes, *SlGT11* plays a role in the differentiation of floral organs, and overexpression of *SlGT11* in transgenic tomatoes results in shorter internodes and smaller leaves [54]. Based on RNA-Seq data, we found that trihelix TFs play specific and significant roles in the growth and development of watermelon. Several genes exhibited tissue-specific expression patterns. For example, the *Cla97C08G147050* gene had high expression levels in tendrils but lower expression levels in leaves and male flowers. The *Cla97C10G205470* gene exhibited high expression levels only in the roots of the one-true-leaf stage, with low expression in other tissues. Homologous genes typically exhibit similar expression patterns [55]. In this study, the homologous gene pair *Cla97C04G073600* and *Cla97C10G205470* showed similar expression patterns and were clustered together in one branch. Interestingly, another two pairs of homologous genes (*Cla97C01G023690–Cla97C07G131110* and *Cla97C03G058990–Cla97C07G131110*) demonstrated significantly different tissue-specific expression patterns. The specific functions of the TFs encoded by these genes require further investigation.

An increasing number of studies have found that trihelix TFs play important roles in various stress responses. To further explore the role of trihelix TFs in environmental adaptation, we systematically analyzed the expression of trihelix genes in watermelon under biotic and abiotic stresses. Under abiotic stress, Liu et al. discovered that rice *OsGTγ-2* could directly interact with the GT-1 element in the *OsRAV2* promoter. Overexpression of *OsGTγ-2* enhanced seed germination rates, seedling growth, and survival rates under salt stress [56]. In contrast, silencing of this gene resulted in rice plants exhibiting a salt-sensitive phenotype. Downregulation of the *SlGT-26* gene, which belongs to the GT-2 family, resulted in dwarf tomato plants with enhanced drought and salt stress resistance [57]. In this study, under high-salinity treatment, the expression level of the *Cla97C10G2055470* gene was significantly upregulated compared to the control. This result suggested that the *Cla97C10G2055470* gene, a member of the GT-1 family, plays an active role in the adaptation of watermelon to high-salinity conditions (Figure 9). Additionally, we also found that the expression level of the *Cla97C10G197980* gene gradually increased with extended high-temperature treatment, indicating the active involvement of its protein product in the response of watermelon to heat stress (Figure 7).

Watermelon production is increasingly threatened by various pests and diseases, and previous studies have found that trihelix TFs are involved in responses to a variety of biotic stresses. Overexpression of the cotton trihelix family gene *GhGT-3b_A04* in *Arabidopsis* enhanced the plant's resistance to *Verticillium* wilt [58]. The U-box-type E3 ubiquitin ligase PUB23 in kiwifruit can interact with *GT1*, and the expression of *GT1* is upregulated in *PUB23*-silenced plants, enhancing the immune response triggered by pathogen-associated molecular patterns [59]. Other trihelix family genes can be synergistically upregulated to accumulate more compounds, like lignin, to resist the infection and expansion of pathogens [60]. In our study, the *Cla97C06G111030* gene exhibited differential expression patterns under various biotic stresses, suggesting that the *Cla97C06G111030* gene plays a broad role in the response of watermelon to biotic stress. Notably, the expression of the *Cla97C06G127520* gene remained significantly upregulated during SqVYV infection in resistant plants compared to the control (Figure 8). These results suggest that the *Cla97C06G127520* gene may be involved in the molecular response of watermelon to SqVYV, which warrants further study.

5. Conclusions

In the current study, we identified 29 trihelix family genes in watermelon. Through a comprehensive analysis of their physicochemical properties, chromosomal localization, gene structure, phylogenetic relationships, collinearity, and expression patterns under different biotic and abiotic stresses, we have significantly expanded the understanding of the evolutionary history and functional potential of these genes in watermelon. Unlike previous studies in other plant species, our research highlights specific genes that are involved in stress responses unique to watermelon, such as the salt tolerance gene *Cla97C10G2055470* and the resistance gene to *SqVYV* disease *Cla97C06G127520*. These findings not only reveal novel insights into the role of trihelix transcription factors in watermelon but also underscore the potential of these genes for improving watermelon's resilience to environmental stress and disease. The distinct functional roles of these trihelix genes in watermelon, compared to other species, suggest their importance in crop improvement and offer valuable targets for future molecular breeding efforts aimed at enhancing stress resistance in watermelon. The next step is to focus on functional validation of core genes to clarify their response mechanisms under stress conditions, which will lay the theoretical foundation for stress-resistant breeding.

Supplementary Materials: The following supporting information can be downloaded at: https://www.mdpi.com/article/10.3390/horticulturae11030275/s1. Figure S1: Sequence alignment of the trihelix proteins of in watermelon.

Author Contributions: N.Q. conceived the research and designed the experiments. Y.W. performed research, analyzed the data, and wrote the manuscript. H.C. and Z.L. participated in downloading transcriptome sequencing data and helped with the bioinformatics analysis. Y.S. and L.S. analyzed and interpreted the data. N.Q. and Y.W. wrote and modified the manuscript. All authors have read and agreed to the published version of the manuscript.

Funding: This research was supported by the Shanxi Basic Research Program Youth Project (202203021212432).

Data Availability Statement: Data is contained within the article.

Conflicts of Interest: The authors declare no conflict of interest.

References

1. Jin, J.; Tian, F.; Yang, D.C.; Meng, Y.Q.; Kong, L.; Luo, J.; Gao, G. PlantTFDB 4.0: Toward a central hub for transcription factors and regulatory interactions in plants. *Nucleic Acids Res.* **2017**, *45*, D1040–D1045. [CrossRef] [PubMed]
2. Zhou, D.X. Regulatory mechanism of plant gene transcription by GT-elements and GT-factors. *Trends Plant Sci.* **1999**, *4*, 210–214. [CrossRef] [PubMed]
3. Ayadi, M.; Delaporte, V.; Li, Y.F.; Zhou, D.X. Analysis of GT-3a identifies a distinct subgroup of trihelix DNA-binding transcription factors in *Arabidopsis*. *FEBS Lett.* **2004**, *562*, 147–154. [CrossRef] [PubMed]
4. Green, P.J.; Kay, S.A.; Chua, N.H. Sequence-specific interactions of a pea nuclear factor with light-responsive elements upstream of the rbcS-3A gene. *EMBO J.* **1987**, *6*, 2543–2549. [CrossRef]
5. Hiratsuka, K.; Wu, X.; Fukuzawa, H.; Chua, N.H. Molecular dissection of GT-1 from Arabidopsis. *Plant Cell* **1994**, *6*, 1805–1813.
6. Perisic, O.; Lam, E. A tobacco DNA binding protein that interacts with a light-responsive box II element. *Plant Cell* **1992**, *4*, 831–838.
7. Gao, M.J.; Lydiate, D.J.; Li, X.; Lui, H.; Gjetvaj, B.; Hegedus, D.D.; Rozwadowski, K. Repression of seed maturation genes by a trihelix transcriptional repressor in *Arabidopsis* seedlings. *Plant Cell* **2009**, *21*, 54–71. [CrossRef]
8. Osorio, M.B.; Bücker-Neto, L.; Castilhos, G.; Turchetto-Zolet, A.C.; Wiebke-Strohm, B.; Bodanese-Zanettini, M.H.; Margis-Pinheiro, M. Identification and in silico characterization of soybean trihelix-GT and bHLH transcription factors involved in stress responses. *Genet. Mol. Biol.* **2012**, *35*, 233–246. [CrossRef]

9. Yu, C.; Cai, X.; Ye, Z.; Li, H. Genome-wide identification and expression profiling analysis of trihelix gene family in tomato. *Biochem. Biophys. Res. Commun.* **2015**, *468*, 653–659. [CrossRef]
10. Song, A.; Wu, D.; Fan, Q.; Tian, C.; Chen, S.; Guan, Z.; Xin, J.; Zhao, K.; Chen, F. Transcriptome-wide identification and expression profiling analysis of chrysanthemum trihelix transcription factors. *Int. J. Mol. Sci.* **2016**, *17*, 198. [CrossRef]
11. Kaplan-Levy, R.N.; Brewer, P.B.; Quon, T.; Smyth, D.R. The trihelix family of transcription factors—Light, stress and development. *Trends Plant Sci.* **2012**, *17*, 163–171. [CrossRef] [PubMed]
12. Maréchal, E.; Hiratsuka, K.; Delgado, J.; Nairn, A.; Qin, J.; Chait, B.T.; Chua, N.H. Modulation of GT-1 DNA-binding activity by calcium-dependent phosphorylation. *Plant Mol. Biol.* **1999**, *40*, 373–386. [CrossRef] [PubMed]
13. Yoo, C.Y.; Pence, H.E.; Jin, J.B.; Miura, K.; Gosney, M.J.; Hasegawa, P.M.; Mickelbart, M.V. The *Arabidopsis* GTL1 transcription factor regulates water use efficiency and drought tolerance by modulating stomatal density via transrepression of *SDD1*. *Plant Cell* **2010**, *22*, 4128–4141. [CrossRef] [PubMed]
14. Shibata, M.; Breuer, C.; Kawamura, A.; Clark, N.M.; Rymen, B.; Braidwood, L.; Morohashi, K.; Busch, W.; Benfey, P.N.; Sozzani, R.; et al. GTL1 and DF1 regulate root hair growth through transcriptional repression of *ROOT HAIR DEFECTIVE 6-LIKE 4* in *Arabidopsis*. *Development* **2018**, *145*, dev159707. [CrossRef]
15. Xi, J.; Qiu, Y.; Du, L.; Poovaiah, B.W. Plant-specific trihelix transcription factor *AtGT2L* interacts with calcium/calmodulin and responds to cold and salt stresses. *Plant Sci.* **2012**, *185–186*, 274–280. [CrossRef]
16. Luo, J.; Tang, S.; Mei, F.; Peng, X.; Li, X.; Yan, X.; Zeng, X.; Liu, F.; Wu, Y.; Wu, G. *BnSIP1-1*, a trihelix family gene, mediates abiotic stress tolerance and ABA signaling in *Brassica napus*. *Front. Plant Sci.* **2017**, *8*, 44. [CrossRef]
17. Fu, M.; Li, F.; Zhou, S.; Guo, P.; Chen, Y.; Xie, Q.; Chen, G.; Hu, Z. Trihelix transcription factor SlGT31 regulates fruit ripening mediated by ethylene in tomato. *J. Exp. Bot.* **2023**, *74*, 5709–5721. [CrossRef]
18. Liu, H.F.; Zhang, T.T.; Liu, Y.Q.; Liu, R.X.; Zhnag, H.Y.; Rui, L.; Wang, D.R.; Li, C.Y.; Zhang, S.; You, C.X.; et al. The trihelix transcription factor MdSIP1-2 interacts with *MdNIR1* promoter to regulate nitrate utilization in apple. *Environ. Exp. Bot.* **2024**, *220*, 105669. [CrossRef]
19. Wang, Z.; Liu, Q.; Wang, H.; Zhang, H.; Xu, X.; Li, C.; Yang, C. Comprehensive analysis of trihelix genes and their expression under biotic and abiotic stresses in *Populus trichocarpa*. *Sci. Rep.* **2016**, *6*, 36274. [CrossRef]
20. Mo, H.; Wang, L.; Ma, S.; Yu, D.; Lu, L.; Yang, Z.; Yang, Z.; Li, F. Transcriptome profiling of *Gossypium arboreum* during fiber initiation and the genome-wide identification of trihelix transcription factors. *Gene* **2019**, *709*, 36–47. [CrossRef]
21. Xiao, J.; Hu, R.; Gu, T.; Han, J.; Qiu, D.; Su, P.; Feng, J.; Chang, J.; Yang, G.; He, G. Genome-wide identification and expression profiling of trihelix gene family under abiotic stresses in wheat. *BMC Genom.* **2019**, *20*, 287. [CrossRef] [PubMed]
22. Li, J.; Zhang, M.; Sun, J.; Mao, X.; Wang, J.; Wang, J.; Liu, H.; Zheng, H.; Zhen, Z.; Zhao, H.; et al. Genome-Wide characterization and identification of trihelix transcription factor and expression profiling in response to abiotic stresses in rice (*Oryza sativa* L.). *Int. J. Mol. Sci.* **2019**, *20*, 251. [CrossRef] [PubMed]
23. Javed, T.; Shabbir, R.; Ali, A.; Afzal, I.; Zaheer, U.; Gao, S.J. Transcription factors in plant stress responses: Challenges and potential for sugarcane improvement. *Plants* **2020**, *9*, 491. [CrossRef] [PubMed]
24. Lindemose, S.; O'Shea, C.; Jensen, M.K.; Skriver, K. Structure, function and networks of transcription factors involved in abiotic stress responses. *Int. J. Mol. Sci.* **2013**, *14*, 5842–5878. [CrossRef]
25. Abdullah; Faraji, S.; Mehmood, F.; Malik, H.M.T.; Ahmed, I.; Heidari, P.; Poczai, P. The GASA gene family in cacao (*Theobroma cacao*, malvaceae): Genome wide identification and expression analysis. *Agronomy* **2021**, *11*, 1425. [CrossRef]
26. Yu, C.S.; Lin, C.J.; Hwang, J.K. Predicting subcellular localization of proteins for Gram-negative bacteria by support vector machines based on *n*-peptide compositions. *Protein Sci.* **2004**, *13*, 1402–1406. [CrossRef]
27. Chen, C.; Chen, H.; Zhang, Y.; Thomas, H.R.; Frank, M.H.; He, Y.; Xia, R. TBtools: An integrative toolkit developed for interactive analyses of big biological data. *Mol. Plant* **2020**, *13*, 1194–1202. [CrossRef]
28. Bailey, T.L.; Williams, N.; Misleh, C.; Li, W.W. MEME: Discovering and analyzing DNA and protein sequence motifs. *Nucleic Acids Res.* **2006**, *34*, W369–W373. [CrossRef]
29. Waterhouse, A.; Procter, J.; Martin, D.A.; Barton, G.J. Jalview: Visualization and analysisof molecular sequences, alignments, and structures. *BMC Bioinform.* **2005**, *6*, P28. [CrossRef]
30. Kumar, S.; Stecher, G.; Tamura, K. MEGA7: Molecular evolutionary genetics analysis version 7.0 for bigger datasets. *Mol. Biol. Evol.* **2016**, *33*, 1870–1874. [CrossRef]
31. Sinsheimer, J.S.; Little, R.J.A.; Lake, J.A. Rooting gene trees without outgroups: EP rooting. *Genome Biol. Evol.* **2012**, *4*, 821–831. [CrossRef] [PubMed]
32. Wang, Y.; Tang, H.; Debarry, J.D.; Tan, X.; Li, J.; Wang, X.; Lee, T.H.; Jin, H.; Marler, B.; Guo, H.; et al. MCScanX: A toolkit for detection and evolutionary analysis of gene synteny and collinearity. *Nucleic Acids Res.* **2012**, *40*, e49. [CrossRef]
33. Wang, D.; Zhang, Y.; Zhang, Z.; Jiang, Z.; Yu, J. KaKs_Calculator 2.0: A toolkit incorporating gamma-series methods and sliding window strategies. *Genom. Proteom. Bioinform.* **2010**, *8*, 77–80. [CrossRef] [PubMed]

34. Brown, J.; Pirrung, M.; McCue, L.A. FQC Dashboard: Integrates FastQC results into a web-based, interactive, and extensible FASTQ quality control tool. *Bioinformatics* **2017**, *33*, 3137–3139. [CrossRef] [PubMed]
35. Bolger, A.M.; Lohse, M.; Usadel, B. Trimmomatic: A flexible trimmer for illumina sequence data. *Bioinformatics* **2014**, *30*, 2114–2120. [CrossRef]
36. Li, H.; Handsaker, B.; Wysoker, A.; Fennell, T.; Ruan, J.; Homer, N.; Marth, G.; Abecasis, G.; Durbin, R. The sequence alignment/map format and SAMtools. *Bioinformatics* **2009**, *25*, 2078–2079. [CrossRef]
37. Pertea, M.; Pertea, G.M.; Antonescu, C.M.; Chang, T.C.; Mendell, J.T.; Salzberg, S.L. StringTie enables improved reconstruction of a transcriptome from RNA-seq reads. *Nat. Biotechnol.* **2015**, *33*, 290–295. [CrossRef]
38. Varet, H.; Brillet-Guéguen, L.; Coppée, J.Y.; Dillies, M.A. SARTools: A DESeq2- and EdgeR-based R pipeline for comprehensive differential analysis of RNA-seq data. *PLoS ONE* **2016**, *9*, e0157022. [CrossRef]
39. Zhang, Y.; Zhao, M.; Tan, J.; Huang, M.; Chu, X.; Li, Y.; Han, X.; Fang, T.; Tian, Y.; Jarret, R.; et al. Telomere-to-telomere *Citrullus* super-pangenome provides direction for watermelon breeding. *Nat. Genet.* **2024**, *56*, 1750–1761. [CrossRef]
40. Li, H.; Dong, Y.; Chang, J.; He, J.; Liu, Q.; Wei, C.; Ma, J.; Zhang, Y.; Yang, J.Q.; Zhang, X. High-throughput microRNA and mRNA sequencing reveals that microRNAs may be involved in melatonin-mediated cold tolerance in *Citrullus lanatus* L. *Front. Plant Sci.* **2016**, *8*, 01231. [CrossRef]
41. Song, Q.; Joshi, M.; Joshi, V. Transcriptomic analysis of short-term salt stress response in watermelon seedlings. *Int. J. Mol. Sci.* **2020**, *21*, 6036. [CrossRef] [PubMed]
42. Yang, Y.; Mo, Y.; Yang, X.; Zhang, H.; Wang, Y.; Li, H.; Wei, H.; Zhang, X. Transcriptome profiling of watermelon root in response to short-term osmotic stress. *PLoS ONE* **2016**, *11*, e0166314. [CrossRef] [PubMed]
43. Yadav, V.; Wang, Z.; Guo, Y.; Zhang, X. Comparative transcriptome profiling reveals the role of phytohormones and phenylpropanoid pathway in early-stage resistance against powdery mildew in watermelon (*Citrullus lanatus* L.). *Front. Plant Sci.* **2022**, *10*, 1016822. [CrossRef] [PubMed]
44. Yasmeen, E.; Riaz, M.; Sultan, S.; Azeem, F.; Abbas, A.; Riaz, K.; Ali, M.A. Genome-wide analysis of trihelix transcription factor gene family in *Arabidopsis thaliana*. *Pak. J. Agric. Sci.* **2016**, *53*, 439–448.
45. Ma, W.; Yang, D.; Qiu, M.; Gao, J.; Cui, R. Genome-wide identification and expression pattern analysis of the trihelix gene family in cucumber. *Pak. J. Bot.* **2024**, *56*, 1853–1866. [CrossRef]
46. Wang, R.; Hong, G.; Han, B. Transcript abundance of *rml*1, encoding a putative GT1-like factor in rice, is up-regulated by *Magnaporthe grisea* and down-regulated by light. *Gene* **2004**, *324*, 105–115. [CrossRef]
47. Breuer, C.; Kawamura, A.; Ichikawa, T.; Tominaga-Wada, R.; Wada, T.; Kondou, Y.; Muto, S.; Matsui, M.; Sugimoto, K. The trihelix transcription factor GTL1 regulates ploidy-dependent cell growth in the *Arabidopsis* trichome. *Plant Cell* **2009**, *21*, 2307–2322. [CrossRef]
48. Fang, Y.; Xie, K.; Hou, X.; Hu, H.; Xiong, L. Systematic analysis of GT factor family of rice reveals a novel subfamily involved in stress responses. *Mol. Genet. Genom.* **2010**, *283*, 157–169. [CrossRef]
49. Kong, H.; Landherr, L.L.; Frohlich, M.W.; Leebens-Mack, J.; Ma, H.; dePamphilis, C.W. Patterns of gene duplication in the plant *SKP1* gene family in angiosperms: Evidence for multiple mechanisms of rapid gene birth. *Plant J.* **2007**, *50*, 873–885. [CrossRef]
50. Roulin, A.; Auer, P.L.; Libault, M.; Schlueter, J.; Farmer, A.; May, G.; Stacey, G.; Doerge, R.W.; Jackson, S.A. The fate of duplicated genes in a polyploid plant genome. *Plant J.* **2013**, *73*, 143–153. [CrossRef]
51. Zhang, S.; Chen, C.; Li, L.; Meng, L.; Singh, J.; Jiang, N.; Deng, X.W.; He, Z.H.; Lemaux, P.G. Evolutionary expansion, gene structure, and expression of the rice wall-associated kinase gene family. *Plant Physiol.* **2005**, *139*, 1107–1124. [CrossRef] [PubMed]
52. Jain, M.; Tyagi, A.K.; Khurana, J.P. Genome-wide analysis, evolutionary expansion, and expression of early auxin-responsive *SAUR* gene family in rice (*Oryza sativa*). *Genomics* **2006**, *88*, 360–371. [CrossRef] [PubMed]
53. O'Brien, M.; Kaplan-Levy, R.; Tezz, Q.; Sappl, P.; Smyth, D. PETAL LOSS, a trihelix transcription factor that represses growth in *Arabidopsis thaliana*, binds the energysensing SnRK1 kinase AKIN10. *J. Exp. Bot.* **2015**, *9*, 2475–2485. [CrossRef] [PubMed]
54. Yang, L.; Qi, S.; Touqeer, A.; Li, H.; Zhang, X.; Liu, X.; Wu, S. *SlGT11* controls floral organ patterning andbfloral determinacy in tomato. *BMC Plant Biol.* **2020**, *20*, 562. [CrossRef]
55. Paterson, A.H.; Bowers, J.E.; Bruggmann, R.; Dubchak, I.; Grimwood, J.; Gundlach, H.; Haberer, G.; Hellsten, U.; Mitros, T.; Poliakov, A.; et al. The *Sorghum bicolor* genome and the diversification of grasses. *Nature* **2009**, *457*, 551–556. [CrossRef]
56. Liu, X.; Wu, D.; Shan, T.; Xu, S.; Qin, R.; Li, H.; Negm, M.; Wu, D.; Li, J. The trihelix transcription factor *OsGTγ-2* is involved adaption to salt stress in rice. *Plant Mol. Biol.* **2020**, *103*, 545–560. [CrossRef]
57. Li, F.; Chen, G.; Xie, Q.; Zhou, S.; Hu, Z. Down-regulation of *SlGT-26* gene confers dwarf plants and enhances drought and salt stress resistance in tomato. *Plant Physiol. Biochem.* **2023**, *203*, 108053. [CrossRef]
58. Mao, H.; Zhang, W.; Lv, J.; Yang, J.; Yang, S.; Jia, B.; Song, J.; Wu, M.; Pei, W.; Ma, J.; et al. Overexpression of cotton Trihelix transcription factor *GhGT-3b_A04* enhances resistance to Verticillium dahliae and affects plant growth in *Arabidopsis thaliana*. *J. Plant Physiol.* **2023**, *283*, 153947. [CrossRef]

59. Wang, T.; Wang, G.; Zhang, J.; Xuan, J. E3 ubiquitin ligase PUB23 in kiwifruit interacts with trihelix transcription factor GT1 and negatively regulates immune responses against *Pseudomonas syringae* pv. *actinidiae*. *Int. J. Mol. Sci.* **2024**, *25*, 1930. [CrossRef]
60. Liu, Q.; Luo, L.; Zheng, L. Lignins: Biosynthesis and biological functions in plants. *Int. J. Mol. Sci.* **2018**, *19*, 335. [CrossRef]

Disclaimer/Publisher's Note: The statements, opinions and data contained in all publications are solely those of the individual author(s) and contributor(s) and not of MDPI and/or the editor(s). MDPI and/or the editor(s) disclaim responsibility for any injury to people or property resulting from any ideas, methods, instructions or products referred to in the content.